Progress of Theoretical Physics, Vol. 108, No. 3, September 2002

Scaling Behavior of $(N_{\rm ch})^{-1}dN_{\rm ch}/d\eta$ at $\sqrt{s_{NN}} = 130$ GeV by the PHOBOS Collaboration and Its Implication

— *A Possible Explanation Employing the Ornstein-Uhlenbeck Process* —

Minoru Biyajima,[1] Masaru Ide,[1] Takuya Mizoguchi[2] and Naomichi Suzuki[3]

[1] *Department of Physics, Faculty of Science, Shinshu University, Matsumoto 390-8621, Japan*
[2] *Toba National College of Maritime Technology, Toba 517-8501, Japan*
[3] *Matsusho Gakuen Junior College, Matsumoto 390-1295, Japan*

(Received March 22, 2002)

Recently, interesting data concerning $dN_{\rm ch}/d\eta$ in Au-Au collisions [$\eta = -\ln\tan(\theta/2)$] with centrality cuts have been reported from the PHOBOS Collaboration. In most treatment these data are divided by the number of participants (nucleons) in collisions. Instead of this method, we use the total multiplicity $N_{\rm ch} = \int (dN_{\rm ch}/d\eta)d\eta$ and find that there is scaling phenomenon among $(N_{\rm ch})^{-1}dN_{\rm ch}/d\eta = dn/d\eta$ with different centrality cuts at $\sqrt{s_{NN}} = 130$ GeV. To explain this scaling behavior of $dn/d\eta$, we employ a stochastic approach using the Ornstein-Uhlenbeck process with two sources. A Langevin equation is adopted for this explanation. Moreover, comparisons of $dn/d\eta$ at $\sqrt{s_{NN}} = 130$ GeV with that at $\sqrt{s_{NN}} = 200$ GeV are made, and no significant difference is found. A possible method for the detection of the quark-gluon plasma (QGP) through $dN_{\rm ch}/d\eta$ is presented.

§1. Introduction

Recently, interesting data from the PHOBOS Collaboration on $dN_{\rm ch}/d\eta$ [$\eta = -\ln\tan(\theta/2)$][*)]in Au-Au collisions at $\sqrt{s_{NN}} = 130$ GeV have been published.[1)] The authors of Ref. 1) calculated the quantity

$$\frac{1}{\langle N_{\rm part}\rangle/2}\frac{dN_{\rm ch}}{d\eta} = f(\langle N_{\rm part}\rangle,\, N_{\rm coll},\, \eta)\,, \tag{1·1}$$

where $N_{\rm part}$ and $N_{\rm coll}$ represent the number of participants (nucleons) and the number of collision particles in Au-Au collisions. The quantity in Eq. (1·1) depends on the centrality cuts. The intercept $f(N_{\rm part},\, N_{\rm coll},\, \eta = 0)$ is an increasing function of $\langle N_{\rm part}\rangle$.

---

*) Here,

$$y = \frac{1}{2}\ln\frac{E+p_z}{E-p_z} = \frac{1}{2}\ln\left[\frac{\sqrt{1+m^2/p_t^2+\sinh^2\eta}+\sinh\eta}{\sqrt{1+m^2/p_t^2+\sinh^2\eta}-\sinh\eta}\right] = \tanh^{-1}\left(\frac{p_z}{E}\right) \approx -\ln\tan(\theta/2) \equiv \eta\,.$$

$$\eta = \frac{1}{2}\ln\frac{p+p_z}{p-p_z} \text{ and } \quad \frac{dn}{d\eta} = \frac{p}{E}\frac{dn}{dy}\,, \text{ where } \quad \frac{p}{E} = \frac{\cosh\eta}{\sqrt{1+m^2/p_t^2+\sinh^2\eta}}\,.$$

In this paper, instead of Eq. (1·1), we consider the physical quantity

$$\frac{1}{N_{\rm ch}}\frac{dN_{\rm ch}}{d\eta}=\frac{dn}{d\eta}\,, \tag{1·2}$$

where $N_{\rm ch}=\int(dN_{\rm ch}/d\eta)d\eta$ and $\int(dn/d\eta)d\eta=1$. In Fig. 1, three sets of values for $dn/d\eta$ are shown. They suggest that there is scaling behavior among the different sets of $dn/d\eta$ with different centrality cuts. Thus, $dn/d\eta$ can be considered a kind of probability density, because the variable η is a continuous variable. This fact probably implies that a stochastic approach is appropriate in analyses of $dn/d\eta$.*)

The content of the present paper is as follows. In §2, we examine the $dn/d\eta$ scaling. In §3, a stochastic approach is considered as one possible explanation of $dn/d\eta$ scaling. In §4, concrete analyses employing Gaussian distributions obtained from the Ornstein-Uhlenbeck (O-U) process are presented. In the final section, concluding remarks are given. In the Appendix, the Fokker-Planck equation for the O-U process is considered.

§2. Confirmation of $dn/d\eta$ scaling

It is worthwhile to confirm whether $dn/d\eta$ scaling holds. Using the intercepts of $dn/d\eta$ at $\eta=0$ in Fig. 1,

$$\left.\frac{dn}{d\eta}\right|_{\eta=0}=c\approx 0.129\pm 0.005\,, \tag{2·1}$$

we can obtain a relation between $N_{\rm ch}$ and $\langle N_{\rm part}\rangle$ as follows. The intercept at $\eta=0$ can be parameterized as

$$\frac{1}{0.5\langle N_{\rm part}\rangle}\left.\frac{dN_{\rm ch}}{d\eta}\right|_{\eta=0}=A\langle N_{\rm part}\rangle^{\alpha}\,, \tag{2·2}$$

*) From studies of multiparticle dynamics in high energy physics, we have learned that the probability distributions $P(n,\langle n\rangle)$ are functions of n and $\langle n\rangle$. It is known that the KNO scaling functions [2]

$$\lim_{n,\,\langle n\rangle\to\infty}\langle n\rangle P(n)=\psi(z=n/\langle n\rangle)\,,$$

are described by solutions of various Fokker-Planck equations. [3),4)] Moreover, this stochastic description is also seen in QCD. For example, Dokshitzer has calculated the generalized gamma distribution in QCD [5)]

$$P(z=n/\langle n\rangle)\approx\frac{2\mu^2}{z}\frac{(Dz)^{3\mu/2}}{\sqrt{2\mu\gamma}}\exp\left[-(Dz)^{\mu}\right]\,,$$

where z is the KNO scaling variable, μ is given by $1-\gamma=1/\mu$, D is a parameter, and γ is the anomalous dimension in QCD. This is a stationary solution of the following Fokker-Planck equation

$$\frac{\partial P}{\partial t}=-\frac{\partial}{\partial z}\left[\left(d+\frac{1}{2}Q\right)z+bz^{1+\gamma}\right]P+\frac{1}{2}Q\frac{\partial^2}{\partial z^2}[z^2P]\,.$$

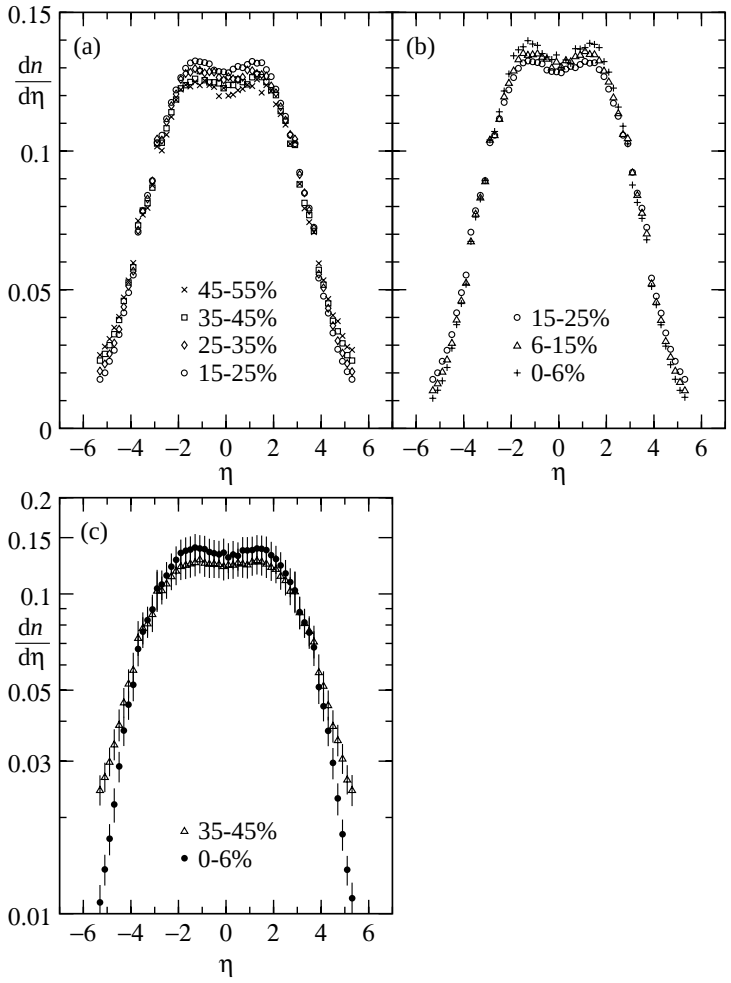

Fig. 1. (a) and (b) Two sets of $dn/d\eta$ with different centrality cuts.[1)] Data with 15–25% are plotted in both figures for the sake of comparison. (c) To examine $dn/d\eta$ in the fragmentation region, a log-linear plot is given.

where $A = 2.16$, and $\alpha = 0.064$. Thus we obtain the relation

$$c = \frac{0.5\langle N_{\rm part}\rangle}{N_{\rm ch}} \frac{1}{0.5\langle N_{\rm part}\rangle} \frac{dN_{\rm ch}}{d\eta}\bigg|_{\eta=0} = \frac{0.5\langle N_{\rm part}\rangle}{N_{\rm ch}} A\langle N_{\rm part}\rangle^{\alpha} . \qquad (2\cdot3)$$

Equation (2·3) is examined in Table I and Fig. 2. That Eq. (2·3) holds approximately among 6 centrality cuts reflects the $dn/d\eta$ scaling, in particular, in the central region.

§3. A possible explanation of $dn/d\eta$ obtained using a stochastic approach

It is well known that the rapidity ($y \approx \eta$) is a kind of velocity. Moreover, there are leading particles in the beam and in target nuclei that collide with each other.

Table I. Empirical examination of Eq. (2·3).

centrality (%)	$2c \times N_{ch}$	$A \times \langle N_{\rm part}\rangle^{1+\alpha}$
35–45	$2 \times 0.129 \times 1056$	$2.16 \times 93^{1+0.064}$
	272.6 ± 14.6	268.5 ± 17.7
25–35	$2 \times 0.129 \times 1582$	$2.16 \times 135^{1+0.064}$
	408.1 ± 21.9	399.1 ± 28.4
15–25	$2 \times 0.129 \times 2270$	$2.16 \times 197^{1+0.064}$
	585.7 ± 31.4	596.7 ± 45.8
6–15	$2 \times 0.129 \times 3199$	$2.16 \times 270^{1+0.064}$
	825.2 ± 44.6	834.5 ± 67.9
0–6	$2 \times 0.129 \times 4070$	$2.16 \times 340^{1+0.064}$
	1050 ± 57	1066 ± 90

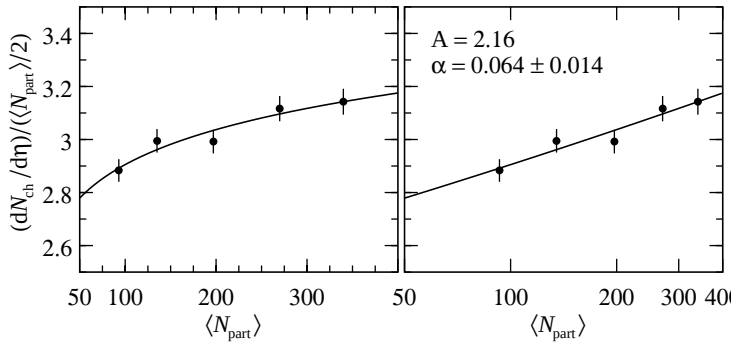

Fig. 2. Determination of the parameters A and α.

For example, nucleons in gold atoms in RHIC experiments collide with each other, and thereby lose energy and emit various particles. Since we have to treat large numbers of particles (e.g., 1k–10k), a stochastic approach seems to be appropriate and to offer a simpler description than Monte Carlo approaches.*)

To describe $dn/d\eta$ scaling with the leading particle effect and fluctuations in rapidity space, we assume the following Langevin equation[8)–10)] for the rapidity variable:**)

$$\frac{dy}{dt} = -\gamma y + f_{\rm w}(t)\,. \tag{3·1}$$

Here t, γ and $f_{\rm w}(t)$ are the evolution parameter,***) the frictional coefficient and a

*) It should be noted that the transport approach is another useful method (see Refs. 6) and 7)).

**) In classical mechanics, Eq. (3·1) corresponds to the equation

$$m\frac{dv}{dt} = -m\gamma v + m f_{\rm w}(t)\,,$$

where v is the velocity.

***) As an alternative interpretation, t may be related to the number of collisions among the wee partons and produced particles.

white noise term, respectively. In our treatment, we assume that $N_{\rm ch}$ particles are produced at $\pm y_{\rm max}$ at $t = 0$. This picture takes into account leading particle effects. Using the assumption $y(0) = \pm y_{\rm max}$, we obtain the solution

$$y(t) = \pm y_{\rm max} e^{-\gamma t} + e^{-\gamma t} \int_0^t e^{\gamma s} f_{\rm w}(s) ds \,. \tag{3·2}$$

The average and variance of $y(t)$ are calculated as

$$E[y(t)] = \pm y_{\rm max} e^{-\gamma t} \,, \tag{3·3}$$

$$E[(E[y(t)] - y)^2] = \frac{\sigma^2}{2\gamma} \left(1 - e^{-2\gamma t}\right) \,, \tag{3·4}$$

where we use the expression

$$\langle f_{\rm w}(t) f_{\rm w}(s) \rangle = \sigma^2 \delta(t - s) \tag{3·5}$$

for the white noise, where σ^2 is the variance. It is known that the distribution function for $y(t)$ is given by a Gaussian distribution with the above average and variance. The probability density with $V^2(t) = (\sigma^2/2\gamma)(1 - e^{-2\gamma t})$ is given by

$$P(y,\, y_{\rm max},\, t) = \frac{1}{\sqrt{8\pi V^2(t)}} \left\{ \exp\left[-\frac{(y + y_{\rm max} e^{-\gamma t})^2}{2V^2(t)} \right] + \exp\left[-\frac{(y - y_{\rm max} e^{-\gamma t})^2}{2V^2(t)} \right] \right\} \,. \tag{3·6}$$

The connection between Eq. (3·1) and the Fokker-Planck equation for the O-U process is given in the Appendix.

In Fig. 3(a), we depict a simplified picture of heavy-ion collision. Our assumptions for the leading particle effect are equivalent to the assumption $P(y,\, y_{\rm max},\, t = 0) = 0.5[\delta(y - y_{\rm max}) + \delta(y + y_{\rm max})]$. In other words, in this model we make the simple assumption that there are two sources of particles at $t = 0$, located at $\pm y_{\rm max}$ and producing $0.5 N_{\rm ch}$ particles each. The evolution of $P(y,\, y_{\rm max},\, t)$ given in Eq. (3·6) is shown in Fig. 3(b).

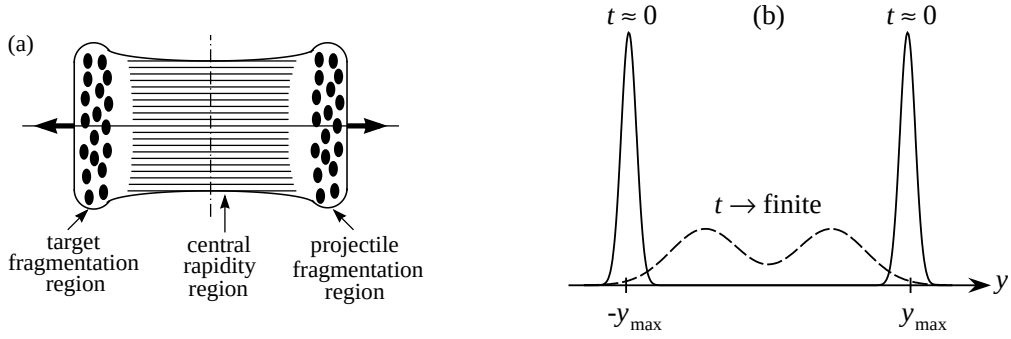

Fig. 3. (a) Simplified picture for A-A collisions. The thin lines represent partons, and the black circles represent nucleons. (b) Evolution of $P(y,\, y_{\rm max},\, t)$ in Eq. (3·6) with two sources at $y_{\rm max}$ and $-y_{\rm max}$.

§4. Analyses of $dn/d\eta$ by means of Eq. (3·6)

Making use of Eq. (3·6), we can analyze $dn/d\eta$ shown in Fig. 1. In our calculation, as most produced particles are not specified, we assume that $y \approx \eta$ in Eq. (3·6). Our results are shown in Fig. 4 and Table II. In Fig. 5, we examine whether or not the variance $V^2(t)$ and the quantity $p = 1 - e^{-2\gamma t}$ depend on the centrality cuts. As is seen in Figs. 3 and 4, the scaling behavior among the sets of $dn/d\eta$ at $\sqrt{s_{NN}} = 130$ GeV is explained by Eq. (3·6), with small changes in the variance $V^2(t)$. The values of $V^2(t)$ depend on the distribution in the fragmentation region $[-\eta_{\max} < \eta < -4$ and $4 < \eta < \eta_{\max}]$. It can be said that the scaling behavior is explained fairly well by the O-U process with two sources, one at the beam ($y_{\rm B}$ or $y_{\max}$) rapidity and one at the target ($y_{\rm T}$ or $-y_{\max}$) rapidity. We have confirmed that an O-U process with

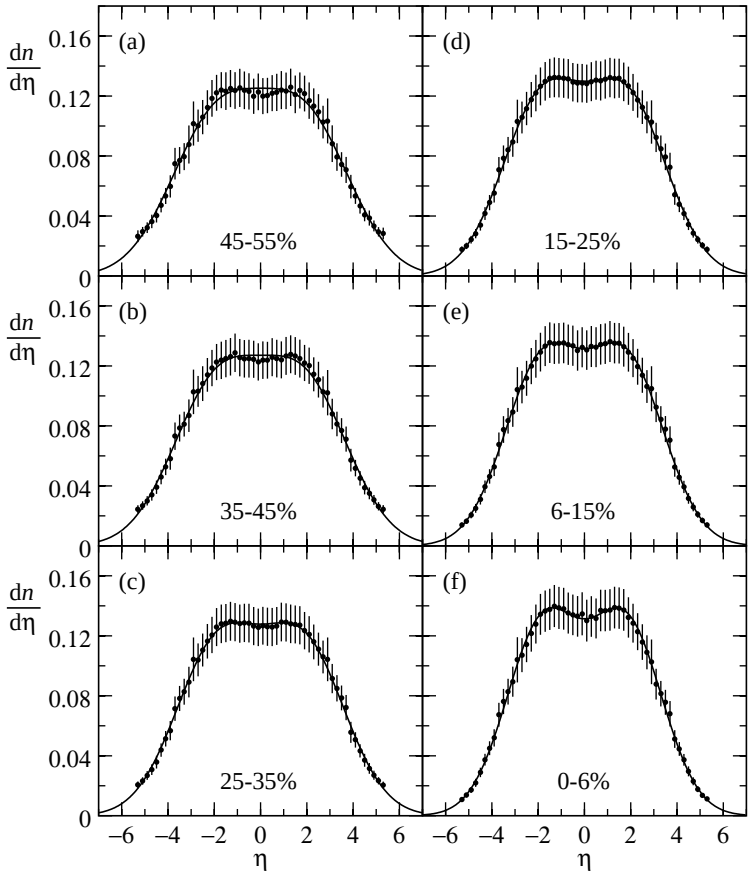

Fig. 4. Analyses of $dn/d\eta$ using Eq. (3·6). (See Table II.)

Table II. Parameter values obtained in our analyses using Eq. (3·6) with two sources. The evolution of $P(y,\, y_{\max},\, t)$ in Eq. (3·6) is stopped at minimum values of χ^2. Here, $\delta p = 0.006 - -0.004$ and $c = \frac{1}{\sqrt{2\pi V^2(t)}} \exp\left[-\frac{(y_{\max}e^{-\gamma t})^2}{2V^2(t)}\right]$. (n.d.f. denotes the number of degree of freedom.)

Fig. 4	(a)	(b)	(c)	(d)	(e)	(f)
centrality (%)	45–55	35–45	25–35	15–25	6–15	0–6
p	$0.872\pm\delta p$	$0.875\pm\delta p$	$0.878\pm\delta p$	$0.882\pm\delta p$	$0.886\pm\delta p$	$0.888\pm\delta p$
$V^2(t)$	3.83±0.27	3.61±0.21	3.23±0.16	3.00±0.13	2.72±0.10	2.47±0.08
$\langle N_{\rm part}\rangle$	—	93	135	197	270	340
$N_{\rm ch}$	662±10	1056±16	1582±23	2270±34	3199±49	4070±63
c	0.125	0.127	0.128	0.130	0.132	0.131
χ^2/n.d.f.	8.61/51	7.63/51	5.88/51	5.35/51	3.57/51	3.82/51

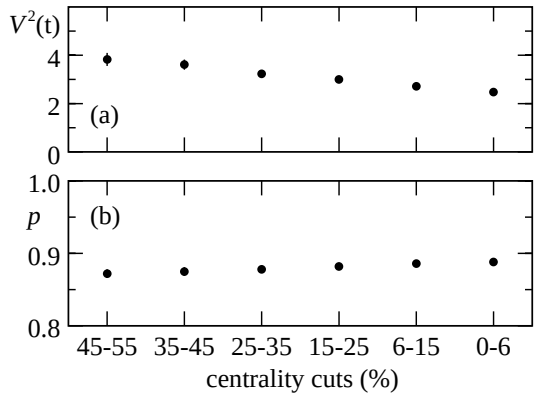

Fig. 5. The values $V^2(t)$ and p of Fig. 4 and Table II.

a single source is not capable of explaining the scaling behavior.*),**)

The intercepts for the sets of $dn/d\eta$ are calculated using the expression

$$c = \frac{1}{\sqrt{2\pi V^2(t)}} \exp\left[-\frac{(y_{\max}e^{-\gamma t})^2}{2V^2(t)}\right]. \tag{4·1}$$

The results are listed in Table II. They are almost the same as the values in Fig. 1.

Here we should carefully examine the values of $V(t)$ in Table II. The slight change reflects the discrepancies in the fragmentation region. As seen in Fig. 1(c), there are small differences in the sets of $dn/d\eta$ for $|\eta| \gtrsim 4$ between the 0–6% centrality cut and the other centrality cuts. To explore the differences more carefully, we need

*) For an explanation with the single source at $y_0 \approx 0$, we can use Eq. (A·2) in the Appendix. For the centrality cut 0–6%, we obtain $\chi^2 = 25.76$, with $m/p_t = 1.3 \pm 0.1$, which is necessary for the single source model. If m/p_t is ignored, we obtain a worse value of χ^2. Thus we disregard this model.

**) We have investigated whether or not the dip structures at $\eta \approx 0$ can be explained by the Jacobian p/E, and obtained the worse values of χ^2 than those listed in Table II. This fact is probably related to the masses of produced particles that are not measured.

sets of $dn/d\eta$ with smaller centrality cuts, for example 0–3% – 0–5%.*),**)

§5. Concluding remarks

First, it can be said that there is scaling among the different sets of $dn/d\eta$ with various centrality cuts at $\sqrt{s_{NN}} = 130$ GeV, as seen from the nearly constant values of c and the behavior in Figs. 1(a)–(c).

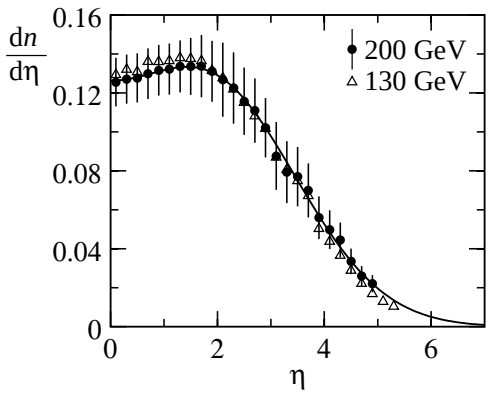

Fig. 6. Comparisons of $dn/d\eta$ with the centrality cut 0–6% at $\sqrt{s_{NN}} = 130$ GeV and 200 GeV. The solid curve is obtained for latter energy. Here $p = 0.879 \pm 0.007$, $V^2(t) = 2.67 \pm 0.24$, χ^2/n.d.f. $= 0.63/22$ and $c = 0.126$.

Second, the scaling behavior of $dn/d\eta$ is described by the solution given in Eq. (3·6) of the Langevin equation with two sources.***)(See Fig. 4 and the values of c in Table II.)

Third, we can add the following fact. Very recently, data for $dN_{\rm ch}/d\eta$ with centrality cut 0–6% at $\sqrt{s_{NN}} =$ 200 GeV from the PHOBOS Collaboration were reported.[16] They are compared with data for $dn/d\eta$ at $\sqrt{s_{NN}} =$ 130 GeV in Fig. 6. From this comparison, it is obvious that the scaling of $dn/d\eta$ holds between $\sqrt{s_{NN}} = 130$ GeV and 200 GeV.†)

Moreover, we can consider the $dn/d\eta$ scaling from a different point of view, i.e., regarding the scaling property

*) A calculation based on QCD is given in Ref. 11) as

$$\frac{2}{\langle N_{\rm part}\rangle}\frac{dN_{\rm ch}}{d\eta}\bigg|_{\eta=0} = a\left(\frac{s}{s_0}\right)^{\lambda/2}\left[\log\left(\frac{Q_{0\rm S}^2}{\Lambda_{\rm QCD}}\right) + \frac{\lambda}{2}\log\left(\frac{s}{s_0}\right)\right],$$

where $a \approx 0.82$, $\Lambda_{\rm QCD} = 0.2$ GeV and $\lambda = 0.25$, and the centrality dependence of the saturation scale is $Q_{0\rm S}^2$. In the fragmentation region, this expression needs cutoff factors.

**) Very recently, the results for $dn/d\eta$ at $\sqrt{s_{NN}} = 130$ GeV and 200 GeV with centrality cuts 0–5% and others obtained by the BRAHMS Collaboration[12),13)] were reported. We have analyzed them using Eq. (3·6) and obtained an almost constant value of $V^2(t)$, because data in the fragmentation region are lacking for $|\eta| \gtrsim 4.5$.

***) To estimate the "thermalization time" of the QGP, Hwa has considered the Fokker-Planck equation for the motion of quarks and gluons in nuclei.[14] (See also Ref. 15), in which the Wiener process is considered for the problem of the thermalization of quarks and gluons.)

†) Using Bjorken's picture[17] for the calculation of the energy density for $|\Delta\eta| \le 0.5$ with a geometrical picture of gold ($R_\tau \approx 6$–7 fm, $c\tau_0 \approx 1$–2 fm, $V \approx \pi R_{\rm T}^2(c\tau_0) \approx 300$ fm^3), we obtain the following values:

$$\varepsilon \sim \frac{3}{2}\frac{1}{V}\frac{dN_{\rm ch}}{d\eta}E_{\rm T}\bigg|_{|\Delta\eta|\le 0.5} \sim 1 \text{ GeV/fm}^3 \quad (130 \text{ GeV}),$$

$$\varepsilon \sim 1.2 \text{ GeV/fm}^3 \quad (200 \text{ GeV}).$$

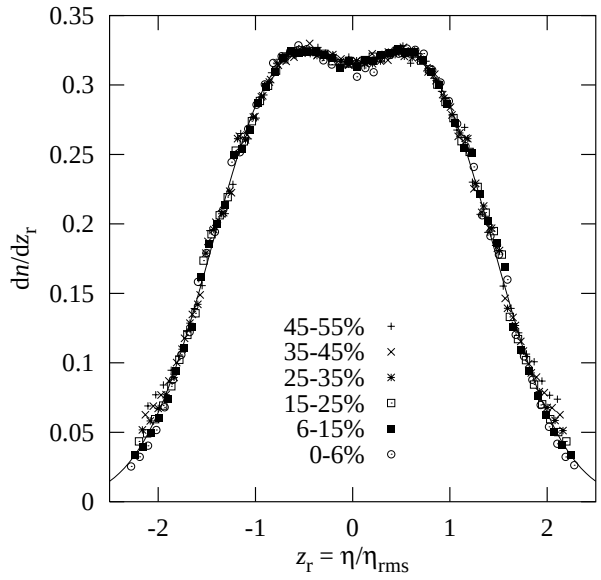

Fig. 7. Normalized distribution of dn/dz_r with $z_r = \eta/\eta_{\rm rms}$ scaling. The solid curve is obtained by $\frac{dn}{dz_r} = \frac{1}{\sqrt{8\pi V_r^2(t)}}\left\{\exp\left[-\frac{(z_r+z_{\max}e^{-\gamma t})^2}{2V_r^2(t)}\right] + \exp\left[-\frac{(z_r-z_{\max}e^{-\gamma t})^2}{2V_t^2(t)}\right]\right\}$, $z_{\max} = 2.23$, $V_r^2(t) = 0.502$, $\chi^2/\text{n.d.f.} = 92.9/321$.

Table III. Values of $\eta_{\rm rms}$ at $\sqrt{s_{NN}} = 130$ GeV.

Fig. 4	(a)	(b)	(c)	(d)	(e)	(f)
centrality (%)	45–55	35–45	25–35	15–25	6–15	0–6
$\eta_{\rm rms} = \sqrt{\langle\eta^2\rangle}$	2.52	2.49	2.45	2.41	2.37	2.33

of Gaussian distributions. Using $\eta_{\rm rms} = \sqrt{\langle\eta^2\rangle} = \sqrt{\sum \eta^2 dn/d\eta}$, we can compute the following quantity with $z_r = \eta/\eta_{\rm rms}$:

$$\eta_{\rm rms}\frac{dn}{d\eta} = \frac{dn}{dz_r} = f(z_r = \eta/\eta_{\rm rms})\,. \tag{5·1}$$

In Fig. 7, we display our result for Eq. (5·1) and give $\eta_{\rm rms}$ in Table III. This scaling of $f(z_r = \eta/\eta_{\rm rms})$ reflects the fact that the sets of $dn/d\eta$ are described by a Gaussian distribution. In other words, the description of $dn/d\eta$ using the O-U process is appropriate.

This $dn/d\eta$ scaling suggests that $dn/d\eta$ with the centrality cut 0–6% does not exhibit singular or particular phenomena related to signatures of the quark-gluon plasma (QGP).*)Of course, care must be taken when handling averaged quantities in statistics. Thus, while at present, it appears that the QGP is not created, it is possible that the QGP is created but its signature is washed out by strong interactions between hadrons.**)

*) From studies of the HBT effect at RHIC, the authors of Ref. 18) have concluded that the expected large radius from the QGP is not observed.

**) Through the measurement of v_2 (flow of nucleons), some physicists have conjectured that

To investigate particular phenomena, like the turbulence and/or deflagration in $dN_{\rm ch}/d\eta$, we need to analyze a single event with smaller centrality cut than 0–6%.

Furthermore, event-by-event analyses using intermittency [21)–26)] and wavelets [27)] are necessary to investigate the detection of QGP and a disoriented chiral condensate (DCC). For the latter case, the ratio of neutral pions ($\langle\pi^0\rangle$) to charged pions ($\langle\pi^{\rm ch}\rangle$), $\langle\pi^0\rangle/\langle\pi^{\rm ch}\rangle$, should be measured. These methods should be applied to $dN_{\rm ch}/d\eta$ with smaller centrality cuts and larger particles. They seem to be capable of extracting useful information on QGPs and DCCs from the analysis of single events.

Finally, we should mention the results of recent analyses of data concerning $dN_{\rm ch}/d\eta$ carried out by the NA50 Collaboration.[28)] It has been reported that there is η-scaling of $dN_{\rm ch}/d\eta$ in the data obtained from Pb + Pb collisions at SPS.[28)] This behavior can be described by a single Gaussian distribution. (See Eq. (A·2).) This fact suggests that the stochastic approach can be used to describe the behavior of $dN_{\rm ch}/d\eta$ at SPS. The intercepts at $\eta_{\rm max}$, $(N_{\rm max})^{-1}dN_{\rm ch}/d\eta = dn/d\eta$ are in range 0.246–0.266 for 6 centrality cuts. It should be noticed that there is no dip structure. Their observation supports the validity of our stochastic approach.

Acknowledgements

One of authors (M. B.) is partially supported by a Grant-in-Aid from the Ministry of Education, Science, Sports and Culture, Japan (No. 09440103). Useful conversations with G. Wilk, T. Osada and S. Raha are gratefully acknowledged.

Appendix A

—— Solution of the Fokker-Planck Equation for the O-U Process ——

The Fokker-Planck equation for the O-U process connected with Eq. (3·1) is given by

$$\frac{\partial P(y,\,t)}{\partial t} = \gamma\left[\frac{\partial}{\partial y}y + \frac{1}{2}\frac{\sigma^2}{\gamma}\frac{\partial^2}{\partial y^2}\right]P(y,\,t)\,. \tag{A·1}$$

The solution of Eq. (A·1) with $P(y,\,0) = \delta(y - y_0)$ is obtained as

$$P(y,\,t) = \frac{1}{\sqrt{2\pi V^2(t)}}\exp\left[-\frac{(y - y_0e^{-\gamma t})^2}{2V^2(t)}\right]\,, \tag{A·2}$$

where we have used a resolution method for partial differential equations, including the equation of the characteristic.[29)] Similarly, the solution of Eq. (A·1) with $P(y,\,0) = 0.5[\delta(y + y_{\rm max}) + \delta(y - y_{\rm max})]$ is obtained as

$$P(y,\,y_{\rm max},\,t) = \frac{1}{\sqrt{8\pi V^2(t)}}\left\{\exp\left[-\frac{(y + y_{\rm max}e^{-\gamma t})^2}{2V^2(t)}\right]\right.$$

the increasing value of v_2 reflects the effect from the compression of nuclear matter.[19)] (See also Ref. 20).)

$$+\exp\left[-\frac{(y-y_{\max}e^{-\gamma t})^2}{2V^2(t)}\right]\Bigg\}\,. \qquad \text{(A·3)}$$

References

1) B. B. Back et al. [PHOBOS Collaboration], Phys. Rev. Lett. **87** (2001), 102303.
2) Z. Koba, H. B. Nielsen and P. Olesen, Nucl. Phys. B **40** (1972), 317.
3) M. Biyajima, Phys. Lett. **137B** (1984), 225 [Addenda; **140B** (1984), 435].
4) M. Biyajima, Phys. Lett. B **139** (1984), 93.
See Also, P. Carruthers and C. C. Shih, Int. J. Mod. Phys. A **2** (1987), 1447.
5) Y. L. Dokshitzer, Phys. Lett. B **305** (1993), 295.
6) S. A. Bass, Nucl. Phys. A **698** (2002), 164.
7) Z. w. Lin, S. Pal, C. M. Ko, B. A. Li and B. Zhang, Phys. Rev. C **64** (2001), 011902.
8) N. G. van Kampen, *Stochastic Processes in Physics and Chemistry* (North-Holland Publ., Amsterdam, 1981).
9) K. Saitou, *Probability and Stochastic Process for Engineers* (in Japanese), (Saiensu-Sya, Tokyo, 1980).
10) J. Hori, *Langevin Equation* (in Japanese), (Iwanami-Shoten, Tokyo, 1982).
11) D. Kharzeev and E. Levin, Phys. Lett. B **523** (2001), 79.
12) I. G. Bearden et al. [BRAHMS Collaborations], Phys. Lett. B **523** (2001), 227.
13) I. G. Bearden et al. [BRAHMS Collaboration], Phys. Rev. Lett. **88** (2002), 202301.
14) R. C. Hwa, Phys. Rev. D **32** (1985), 637.
15) S. Chakraborty and D. Syam, Lett. Nuovo Cim. **41** (1984), 381.
See also, J. Alam, B. Sinha and S. Raha, Phys. Rev. Lett. **73** (1994), 1895.
16) B. B. Back et al. [PHOBOS Collaboration], Phys. Rev. Lett. **88** (2002), 022302.
17) J. D. Bjorken, Phys. Rev. D **27** (1983), 140.
18) C. Adler et al. [STAR Collaboration], Phys. Rev. Lett. **87** (2001), 182301.
19) K. H. Ackermann et al. [STAR Collaboration], Phys. Rev. Lett. **86** (2001), 402.
20) T. Hirano, Phys. Rev. C **65** (2002), 011901.
21) T. H. Burnett et al., Phys. Rev. Lett. **50** (1983), 2062.
22) F. Takagi, Phys. Rev. Lett. **53** (1984), 427.
23) A. Bialas and R. Peschanski, Nucl. Phys. B **273** (1986), 703.
24) M. Biyajima, A. Bartl, T. Mizoguchi and N. Suzuki, Phys. Lett. B **237** (1990), 563 [Addenda; B **247** (1990), 629].
25) I. V. Andreev, M. Biyajima, I. M. Dremin and N. Suzuki, Int. J. Mod. Phys. A **10** (1995), 3951.
26) R. C. Hwa, *Quark-Gluon Plasma* (World Scientific, Singapore, 1990), p. 665.
27) N. Suzuki, M. Biyajima and A. Ohsawa, Prog. Theor. Phys. **94** (1995), 91.
See also, N. Suzuki, M. Biyajima and A. Ohsawa, Nucl. Phys. Proc. Suppl. **52B** (1997), 246.
28) M. C. Abreu et al. [NA50 Collaboration], Phys. Lett. B **530** (2002), 33; ibid. **530** (2002), 43.
See also, M. Biyajima et al., Soryushiron Kenkyu (Kyoto) **105** (2002), A117. It should be noticed that those analyses have been made before the publication of NA50 Collaboration.
29) N. S. Goel and N. Richter-Dyn, *Stochastic Models in Biology* (Academic Press, New York, 1974).
30) G. Wolschin, Eur. Phys. J. A **5** (1999), 85.

Note added in proof: After completion of this paper, we are informed that the relativistic diffusion model has been used for analysis of the proton distributions in heavy ion collisions by Wolschin.[30] A similar Fokker-Planck equation is used therein.